Acta Biomaterialia 8 (2012) 1490–1497

Contents lists available at SciVerse ScienceDirect

Acta Biomaterialia

journal homepage: www.elsevier.com/locate/actabiomat

Development of micropatterned surfaces of poly(butylene succinate) by micromolding for guided tissue engineering

Daniela F. Coutinho [a,b], Manuela E. Gomes [a,b], Nuno M. Neves [a,b], Rui L. Reis [a,b,*]

[a] 3B's Research Group – Biomaterials, Biodegradables and Biomimetics, Department of Polymer Engineering, University of Minho, Headquarters of the European Institute of Excellence on Tissue Engineering and Regenerative Medicine, AvePark, Taipas, 4806-909 Guimarães, Portugal
[b] ICVS/3B's – PT Government Associate Laboratory, Braga/Guimarães, Portugal

ARTICLE INFO

Article history:
Received 30 September 2011
Received in revised form 29 November 2011
Accepted 30 December 2011
Available online 8 January 2012

Keywords:
Poly(butylene succinate)
Micromolding
Microfeatures
Human adipose stem cells

ABSTRACT

Native tissues present complex architectures at the micro- and nanoscale that dictate their biological function. Several microfabrication techniques have been employed for engineering polymeric surfaces that could replicate in vitro these micro- and nanofeatures. In this study, biomimetic surfaces of poly(butylene succinate) (PBS) were engineered by a micromolding technique. After the optimization of the system parameters, 20 surfaces with different combinations of groove and ridge sizes were developed and characterized by scanning electron microscopy (SEM). The influence of the engineered microfeatures over the viability and attachment of human adipose derived adult stem cells (hASCs) was evaluated. hASCs cultured onto the engineered surfaces were demonstrated to remain viable for all tested patterns. SEM and immunostaining showed adequate attachment and spreading of the stem cells for all the patterned groove/ridge combinations. This study indicated that it is possible to engineer micropatterned surfaces of PBS and that the developed structures could have great potential for tissue engineering where cell alignment is an essential requisite.

1. Introduction

One of the major motivations for the increasing effort spent on designing and developing micro- and nanostructured surfaces and materials for tissue engineering strategies is that natural tissues and the associated extracellular matrices (ECMs) are composed of micro- and nanoscaled elements [1,2]. In fact, when an implant first contacts the host environment, a layer of proteins immediately covers the surface of the implant [3]. The adsorptive behavior of these proteins is highly dependent on the surface properties, including its micro- and nanostructure [4,5], as well as on the material chemistry [6,7]. This surface-specific adjustment can result in the presentation of different regions of the proteins to cells, ultimately determining the success of the implant.

The micro- and nanoscale biological elements present in the ECM arrange themselves in specific architectures, essential for normal tissue function. An outstanding example is the organization of fibroblasts and cardiomyocytes in native myocardial tissue. These cells align themselves and assemble in parallel arrays in a way that is critical to obtain the electrical and mechanical properties of the heart [8]. Similarly, collagen fibers in the bone are aligned structures that provide bone with the tensile strength necessary to ensure the functionality of the tissue [9]. Thus, while developing engineered tissues it is of major importance to replicate the native microarchitecture, namely the controlled cellular alignment, and therefore to modulate in vitro the tissue function.

Several microfabrication techniques allow replication of the microarchitecture of tissues, modulating in vitro the cell shape, function or differentiation. Specifically, several different methods have been reported for cellular alignment, namely micropatterning of molecules [10], fabricating fibrous scaffolds by electrospinning [11–13] or engineering microchannels using soft-lithography methodologies [14,15]. Substrates with micropatterned adhesive proteins provide tight control over the cell attachment process. However, these patterned surfaces consist of a two-dimensional (2-D) substrate to culture cells. Three-dimensional (3-D) structures with multiple opportunities for cell attachment have been developed using various technologies, including electrospinning [11–13]. It has been reported that cells are able to align along the fibers within the 3-D network [12]. In order to more precisely control the overall orientation of cells, microchannels have been fabricated using micromolding or photolithography methods. Cardiac organoids have been formed within microengineered channels as a result of the alignment of cardiomyocytes [14].

* Corresponding author at: 3B's Research Group – Biomaterials, Biodegradables and Biomimetics, Department of Polymer Engineering, University of Minho, Headquarters of the European Institute of Excellence on Tissue Engineering and Regenerative Medicine, AvePark, Taipas, 4806-909 Guimarães, Portugal. Fax: +351 253 510909.
E-mail address: rgreis@dep.uminho.pt (R.L. Reis).

1742-7061/$ - see front matter © 2012 Acta Materialia Inc. Published by Elsevier Ltd. All rights reserved.
doi:10.1016/j.actbio.2011.12.035

In this work we report a simple method to control the alignment of human adipose stem cells (hASCs) by microengineering the surface of a poly(butylene succinate) (PBS) polymeric surface. PBS is an aliphatic polyester that has shown to be biodegradable [16,17]. It has been processed by our group into discs [18] and fibers [19], showing promising results for bone [20] and cartilage [21] tissue engineering, both in vitro [19,21] and in vivo [20]. Herein, a micromolding technique was employed to fabricate microfeatures with different groove/ridge sizes onto the polyester PBS surface. This system can be used as an in vitro model for the study of the biological performance of cells in different patterned surfaces. The described system is applicable to a variety of cell types, and it might prove possible to incorporate the lessons learnt from this system into device design of engineered tissues with specific cell shape and elongation in vitro, as observed in collagen fibers in bone.

2. Experimental

2.1. Materials and solutions

The polymeric material used for the preparation of the substrates in this study was commercially available PBS (Bionolle 1050, Showa High Polymer Co. Ltd., Tokyo, Japan). Substrates for the micropatterns of PBS were processed into circular discs (10 mm diameter, 1.5 mm height) by conventional injection molding technology using optimized processing conditions, as described elsewhere [18]. For the development of the patterns, PBS pellets were dissolved at 0.5% and 2% (w/v), with a pure solvent of either dichloromethane (DIM, Sigma) or trichloromethane (TIM, VWR). A polydimethylsiloxane (PDMS) mold was kindly provided by Professor Hong Hong Lee (School of Chemical Engineering, Seoul National University). The PDMS mold was fabricated with 20 patterns with various combinations of groove and ridge sizes, enabling the effect of a range of scales of the patterns on the biological activity of cells on those substrates to be determined.

2.2. Preparation of micropatterned PBS surfaces

The PDMS mold and the PBS polymeric solution were heated to the same temperature. 20 μl of PBS solution were pipetted on top of the pattern present on the PDMS mold. An injection-molded disc of PBS was placed over the PBS solution as a substrate for the PBS pattern. A weight was used to facilitate the migration of the PBS solution by capillarity through the PDMS micropatterns. As the solvent evaporates (~2 min), the micropatterns of the PDMS are transferred to the PBS injection-molded discs (substrate) and the PBS disc is gently removed from the surface of the PDMS mold (Fig. 1). Three parameters of the system were varied in order to evaluate their influence over the fabricated microfeatures: (i) the temperature of both the PDMS mold and the PBS solution (~20 and ~100 °C); (ii) the concentration of the PBS solution (0.5% and 2%, w/v); and (3) the solvent used to dissolve PBS pellets (DIM or TIM). Twenty patterns with different groove/ridge size combinations were fabricated. Micropatterned PBS surfaces were analyzed by scanning electron microscopy (SEM) using a Leica Cambridge S-360 (Leica Cambridge, UK). All specimens were precoated with a conductive layer of sputtered gold. SEM micrographs were taken at an accelerating voltage of 15 kV at a number of magnifications. The width of the grooves and ridges of the patterns was calculated using an image analysis software (NIH Image J, $n = 4$). The depth of the grooves was constant for all micropatterns (~1.2 μm). Six PBS micropatterns from the 20 developed were selected for further biological studies (Nos. 3, 4, 6, 8, 15, 20) to obtain a good coverage of the range of dimensions that may have a stronger effect over the cells.

2.3. Attachment and proliferation of human adipose stem cells

2.3.1. Cell culture

In order to observe the cell response on the micropatterned PBS surfaces, primary hASCs were seeded on the engineered surfaces. hASCs were isolated as described elsewhere [22]. Briefly, stem cells were isolated from human adipose tissue samples by the enzymatic digestion of the tissue with 0.2% collagenase type IA in phosphate-buffer saline (PBS, Sigma) for 60 min at 37 °C under gentle stirring. Digested tissue was filtered and adherent cells selected after centrifugation steps. Cells were expanded in Dulbecco's Modified Eagle's Medium (DMEM, Sigma) supplemented with 10% heat-inactivated fetal bovine serum (FBS, Biochrom AG) and 1% antibiotic (Gibco) at 37 °C in a humidified atmosphere with 5% CO_2 until a sufficient number for the study was obtained. Three samples per pattern were placed in 24-well plates and 1.5 ml of the cell suspension was seeded onto the PBS micropatterned surfaces using a density of 3.3×10^4 cells ml^{-1}. Seeded cells were incubated in a humidified atmosphere at 37 °C and 5% of CO_2 for 1 and 3 days in order to evaluate cell morphology upon spreading. TCPS was used as a control surface.

2.3.2. Cell viability assay

Cell viability was evaluated during culture time (1 and 3 days) by quantifying the metabolic activity of hASCs, using Alamar Blue® (Invitrogen). Alamar Blue can be reduced in active cell mitochondria, changing the solution color from blue to a bright red. Alamar Blue stock solution was diluted with culture medium without phenol red. Analysis was performed according to the manufacturer's

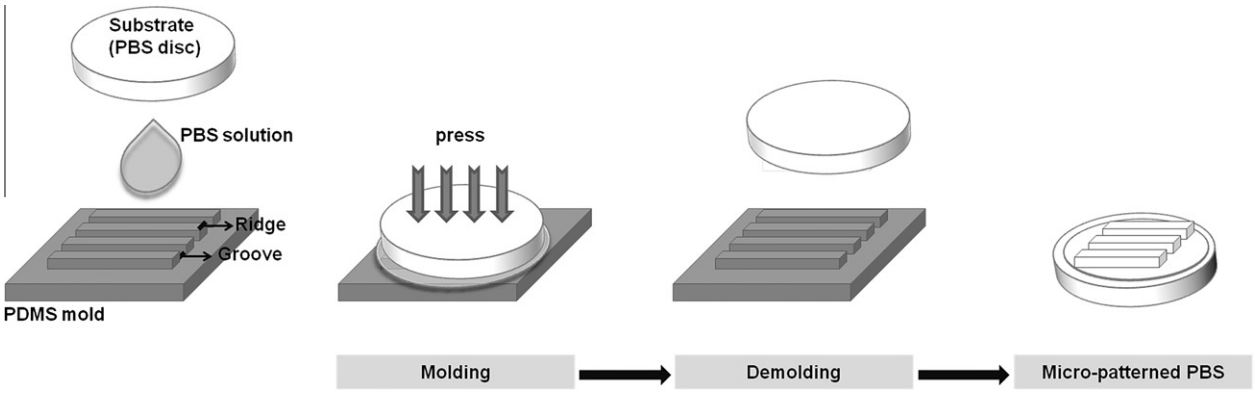

Fig. 1. Schematic representation of the preparation of micropatterned PBS surface.

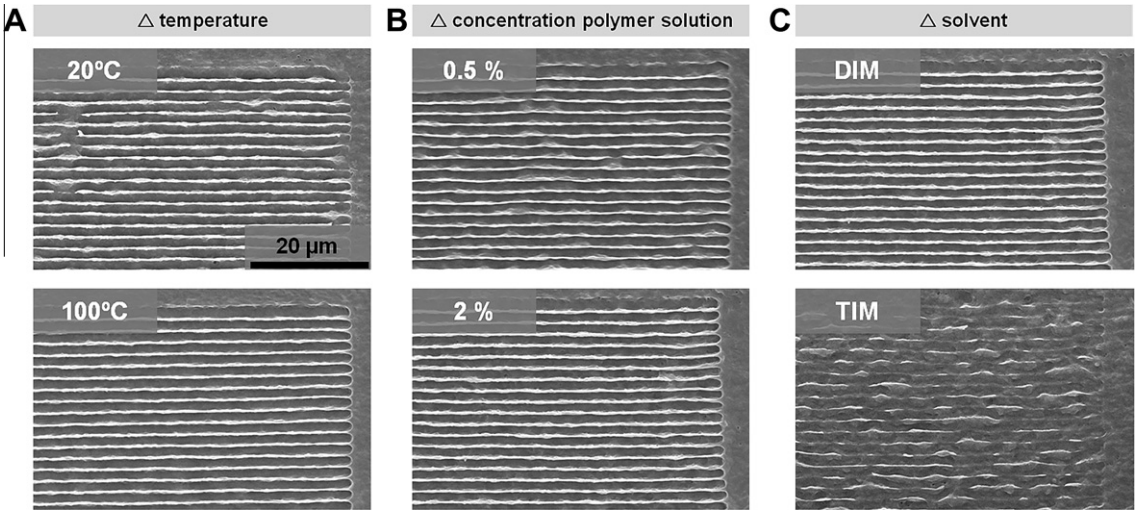

Fig. 2. Influence of the various process parameters on the fabrication of PBS microfeatures. SEM of PBS microfeatures using (A) two different temperatures, (B) two different polymer concentrations and (C) two different solvents.

instructions. The plates were exposed to an excitation wavelength of 540–570 nm and the emission at 580–610 nm recorded in a microplate ELISA reader (BioTek, USA). The percentage viability was expressed as the fluorescence measured in patterned surfaces in comparison to the non-patterned PBS surface.

2.3.3. DNA quantification

After each time-point, cells were lysed by osmotic and thermal shock and the supernatant used for DNA analysis. Cell proliferation was evaluated by quantifying the DNA content on the samples using a PicoGreen dsDNA kit (Molecular Probes). Analysis was performed according to the manufacturer's instructions. Fluorescence was read (485/528 nm excitation/emission) in a microplate ELISA reader (BioTek). The DNA amount was calculated from a standard curve.

2.3.4. Cell morphology analysis

After each incubation period, samples were washed with PBS solution, fixed with 4% formaldehyde (Merck) and kept at 4 °C in PBS solution until they were prepared for SEM or immunostaining. For SEM analysis samples were dehydrated using graded ethanol solutions (50, 70, 90 and 100%, v/v). Immunostaining was performed to obtain further details about the cell morphology using an Axioplan 2 microscope (Zeiss, Germany). The cell cytoskeletons of cells were stained with phalloidin and the cell nuclei counterstained with DAPI.

2.4. Statistical analysis

All data were subjected to statistical analysis and were reported as mean ± standard deviation. Statistical significance in biological studies was determined by analysis of variance (two-way ANOVA) followed by Bonferroni's post hoc test for multiple comparisons using GraphPad Prism 5 Software. The differences were considered statistically significant if $(^{*,\#})P < 0.05$, $(^{**,\#\#})P < 0.01$ or $(^{***,\#\#\#})P < 0.001$.

3. Results and discussion

3.1. Fabrication of micropatterned PBS surfaces

In this study, micromolding was used to develop micropatterned surfaces in a biodegradable polyester. PBS pellets were dissolved in an organic solvent (DIM or TIM) and 20 µl of the solution was placed over the PDMS mold. Injection-molded discs of PBS, previously fabricated as described elsewhere [18], were used as substrates for the micropatterned PBS surfaces (Fig. 1). The most relevant parameters of the process of micromolding PBS surfaces were varied, while keeping the others constant: (i) the temperature of the mold and of the solution (using DIM as solvent and 1% w/v of polymer solution); (ii) the concentration of the polymeric solution (using DIM as solvent and 100 °C); and (iii) the solvent used to dissolve the PBS pellets (using a 1% w/v polymer solution at 100 °C). The SEM micrographs depicted in Fig. 2A show that higher temperatures (~100 °C) allow the polymeric solution to flow and to fill more easily by capillarity the micropatterns of the mold. The optimization shows that more defined patterns were obtained when the PDMS mold and the PBS solution were at a temperature of 100 °C when compared to 20 °C. Suh et al. first described a technology that consists of a variation of the micromolding methodology, which is based on the flow of the polymeric solution by capillarity of the heated polymer, named capillary force lithography [23–25]. The effect of polymer concentration on the definition of the PBS micropatterns was also evaluated (Fig. 2B). PBS pellets were dissolved at 0.5% and 2% (w/v) in DIM. Interestingly, sharp contours could be observed for both concentrations. It would be expected that the less concentrated solution would flow more easily through the micropatterns of the mold as a result of its lower viscosity. However, no significant difference was observed at the studied length scale (µm). Thus the highest concentration (2%, w/v) was selected for the following studies. The third parameter analyzed was the solvent used to dissolve the PBS pellets (Fig. 2C). Both DIM and TIM can dissolve the studied biodegradable polyester, the former being the less hazardous. Thus, micropatterns were fabricated with solutions of PBS pellets dissolved in both solvents. Sharper edges were observed for the micropatterns fabricated with DIM. Thus, DIM was the solvent selected for the subsequent studies. The evaluated system parameters presented a similar behavior when analyzed with other patterns (data not shown).

Using the optimized parameters of 2% (w/v) solution of PBS pellets dissolved in DIM at 100 °C, it was possible to engineer 20 different micropatterns of PBS with a variety of groove and ridge sizes and groove/ridge ratios. Fig. 3A shows a top view of the PBS micropatterns analyzed by SEM. The majority of the micropatterns show quite defined surface features. However, some of them show the presence of a rough surface both on the grooves and in the

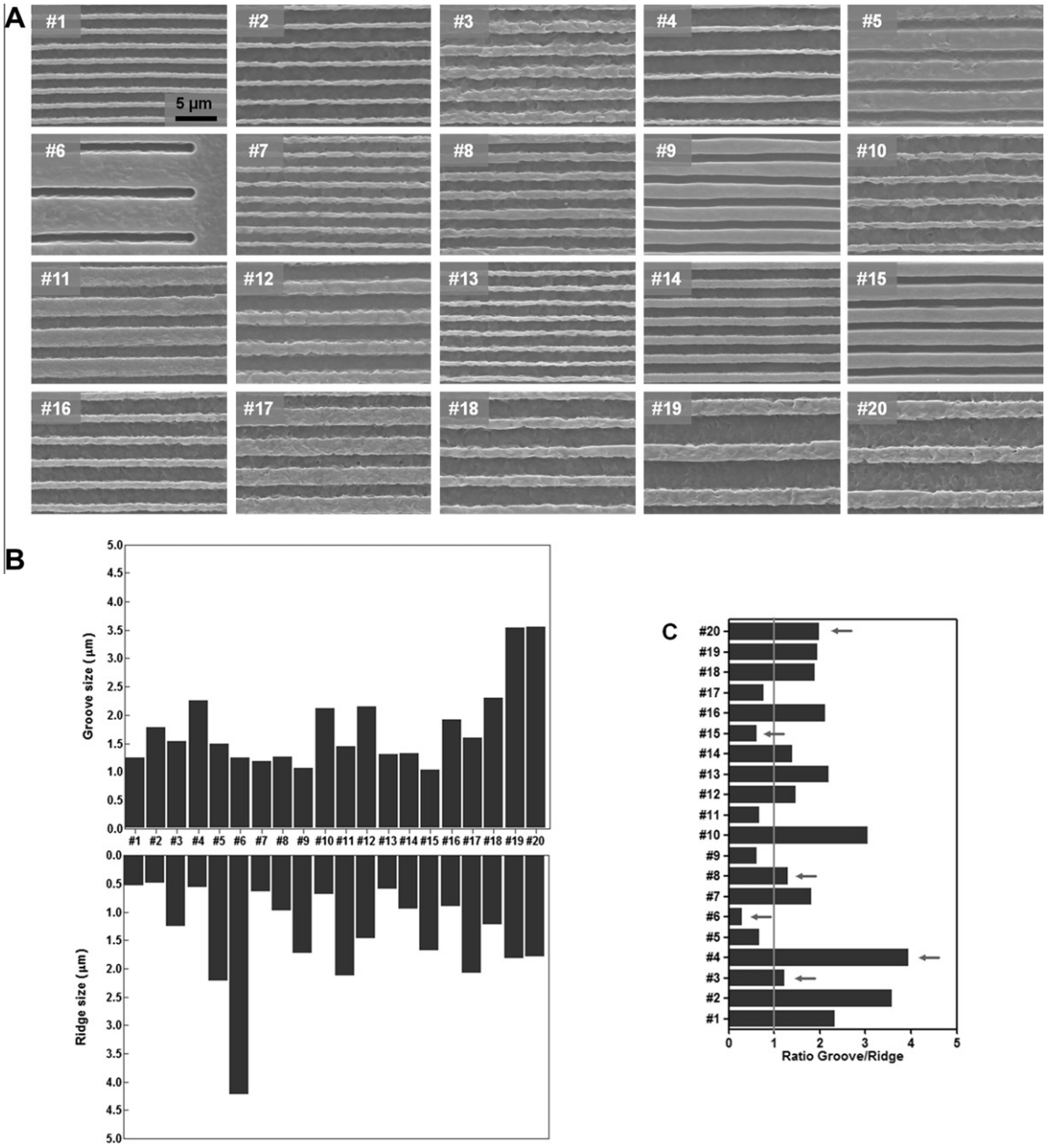

Fig. 3. (A) SEM of PBS microfeatures using 20 different PDMS molds. (B) Dimensions in μm of the groove and ridge of the engineered micropatterns of PBS ($n = 4$) and (C) calculated ratio between the groove and ridge size of the micropatterned PBS surfaces (arrows depict the selected patterns for the biological studies).

ridges of the patterns. The volume of the solution used is small and the percentage of polymer within the total volume corresponds to a small fraction (2%, w/v), being 98% of the volume constituted by the solvent. Given that the solvent quickly evaporates at 100 °C, the creation of a slightly rough structure was expected as observed in Fig. 3A. A variety of micropatterned surfaces has been developed using different methodologies and biomaterials as substrates [26–28]. Laser [26] and UV-based [26] patterning are two exciting alternative methodologies for engineering surfaces with specific patterns. Although these allow structures with higher pattern resolution to be obtained, they usually require quite expensive machinery and complex working environments [29,30]. However, the process herein described allowed the development of micropatterned surfaces using a simple and quite inexpensive system. The downside is a decrease in the resolution of the patterns due to the presence of a rough surface.

The dimensions of the patterns were measured from the SEM micrographs using image analysis software (NIH ImageJ). The groove and ridge sizes of each micropatterned PBS surface are summarized in Fig. 3B. The groove size ranged between 1.0 and 3.5 μm and the ridge size varied from 0.4 to 4.2 μm. Patterns No. 19 and 20 present the highest groove size and pattern No. 6 the highest ridge size. Patterns No. 19 and 20 presented the highest values of both groove and ridge and No. 1 the smallest. The ratio between the groove and ridge sizes was calculated and is shown in Fig. 3C, where it can be seen that 10 patterns had a groove size larger than the ridge size. The different patterns can be approximately organized into three groups: (1) groove size bigger than ridge size ($G > R$, patterns No. 1, 2, 4, 7, 10, 13, 16, 18, 19, 20); (2) groove size smaller than ridge size ($G < R$, patterns No. 5, 6, 9, 11, 15, 17); and (3) similar groove and ridge sizes ($G \approx R$, patterns No. 3, 8, 12, 14). Given these categories, six different patterns were

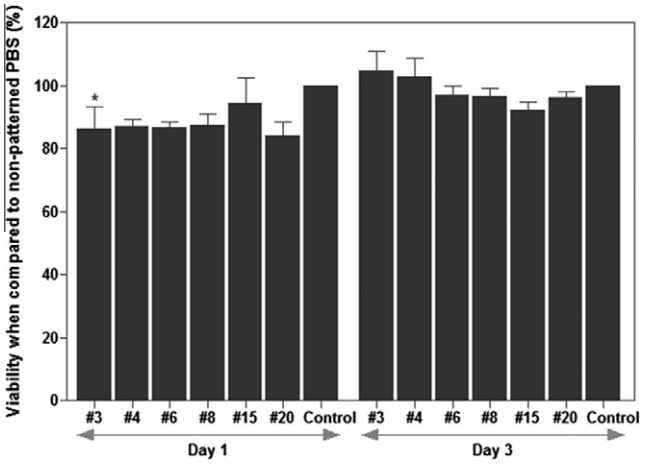

Fig. 4. Viability of hASCs cultured onto micropatterned PBS surfaces after 1 and 3 days of culture ($^{*}P < 0.05$ when compared to day 3).

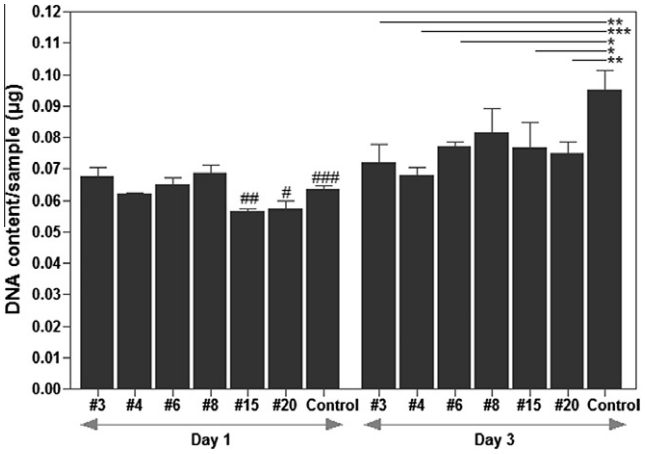

Fig. 5. DNA content of hASCs cultured onto micropatterned PBS surfaces after 1 and 3 days of culture (control corresponds to the non-patterned PBS surface, significantly different samples: $^{\#}P < 0.05$, $^{\#\#}P < 0.01$, $^{\#\#\#}P < 0.001$ when compared to the respective surface at day 3; $^{*}P < 0.05$, $^{**}P < 0.01$, $^{***}P < 0.001$ when compared to the control of day 3).

selected for the biological studies. Patterns No. 3 and 4 were selected since they presented a groove size bigger than the ridge size, the difference being higher for pattern No. 4. Patterns No. 6 and 15 were selected because they presented a groove size smaller than the ridge size, this being difference more pronounced for pattern No. 6. Pattern No. 8 was selected as the pattern with the groove/ridge ratio closest to 1. Finally, pattern No. 20 was also selected since both features were larger than 2 µm, which is more within the range of the size that the cells under study sense with their filopodia [31].

3.2. Cell behavior analysis

The in vitro biological performance of the engineered PBS micropatterned surfaces was assessed after cell culture with hASC. Fig. 4 shows the viability of cultured hASCs when compared to non-patterned PBS surfaces (control, 100%). It is significant that the viability of hASC was similar for all patterned and non-patterned surfaces for both time-points. As an exception, pattern No. 3 presented a significantly higher viability on day 3 ($^{*}P < 0.05$). The results showed that hASCs are equally metabolically active in all the engineered and non-engineered surfaces, indicating that the engineered microsurfaces do not influence negatively the mitochondrial metabolic activity of the studied cells.

Quantification of the amount of double-stranded DNA (dsDNA) for different time periods (Fig. 5) suggested that cultured hASCs proliferated from day 1 to day 3 of culture, this increase in DNA content being statistically significant for patterns No. 15 ($^{\#\#}P < 0.01$) and 20 ($^{\#}P < 0.05$), which present similar ridge values, and for the non-patterned PBS surface (control, $^{\#\#\#}P < 0.001$). Although at day 1 no statistically significant difference on the DNA content was observed among the patterns, at day 3 of culture all patterns, with the exception of pattern No. 8, presented a significantly lower DNA content ($^{*}P < 0.05$, $^{**}P < 0.01$, $^{***}P < 0.001$) than non-patterned surfaces, suggesting that hASCs would proliferate better on non-patterned surfaces. The higher DNA content on pattern No. 8 might indicate that hASCs proliferate better on surfaces with a groove/ridge ratio close to 1, meaning that higher cell number might be found in micropatterned surfaces with similar ridge and groove widths. It has been reported that the average doubling time for hASC populations is 60 h [32]. In this study we have analyzed the dsDNA content after 72 h in culture. Thus, although the DNA content is lower in PBS micropatterned surfaces, cells might still be undergoing cell division. These results suggest that hASCs increase their dsDNA content faster on the non-patterned surfaces. However, on the micropatterned surfaces, cells undergo cytoskeletal rearrangement in response to the micropatterned substrate, which might be responsible for delaying the cell division mechanism.

The SEM analysis of the adhered cells after 1 day of culture onto the different micropatterned surfaces provided further information regarding the influence of the micropatterns on the cell morphology (Fig. 6). After 1 day of culture the majority of cells were attached but not spread on the micropatterned and non-patterned PBS surfaces. Cytoskeleton staining of cultured hASC further confirmed the SEM micrographs (Fig. 6Aii). For most of the micropatterned surfaces the red staining of phalloidin overlapped the DAPI staining of the nucleus, indicating that cells were attached but not spread, as the cytoskeleton was not stretched. However, cells appear to spread faster in patterns No. 15 and 20, given that after 1 day in culture the hASCs seem more widely spread on these patterns. After 1 day of culture, hASCs seem to orient on the micropatterned PBS surfaces along the direction of the patterns. On the other hand, on the non-patterned PBS surfaces, hASCs were observed to form a uniform layer. This effect was more obvious after 3 days of culture (Fig. 6B). Cells seemed to elongate more along the micropatterns on the PBS surfaces, this behavior being more obvious on patterns No. 3, 6, 8 and 20. Similarly to day 1 of culture, hASCs appeared to be randomly oriented on the non-patterned PBS surfaces. Phalloidin staining of cell cytoskeleton and counterstaining of the nucleus with DAPI further confirmed the SEM results. The cytoskeleton of hASCs appeared to be especially elongated on patterns No. 3 and 20. Overall, these results suggest that hASCs can align better along the orientation of the micropatterns in those surfaces where the groove width is bigger than the ridge width (patterns No. 3 and 20). However, it seems that there is a lower limit for the ridge width that cells prefer for alignment, given that this behavior is not observed in the pattern where the groove width is much bigger than the ridge width (pattern No. 4). This behavior might be a result of the low value of the ridge width in this pattern when compared with the others.

Our results suggest that hASCs can recognize the size of the patterns engineered on the PBS surfaces and align along their direction. Cells form cytoplasm extensions and cellular associations over different ridges instead of populating the groove of the patterns. This results from the fact that the size of hASCs is within the range of 20–50 µm, while the micropatterns are less than 5 µm wide. It has been reported that cells can align along microfe-

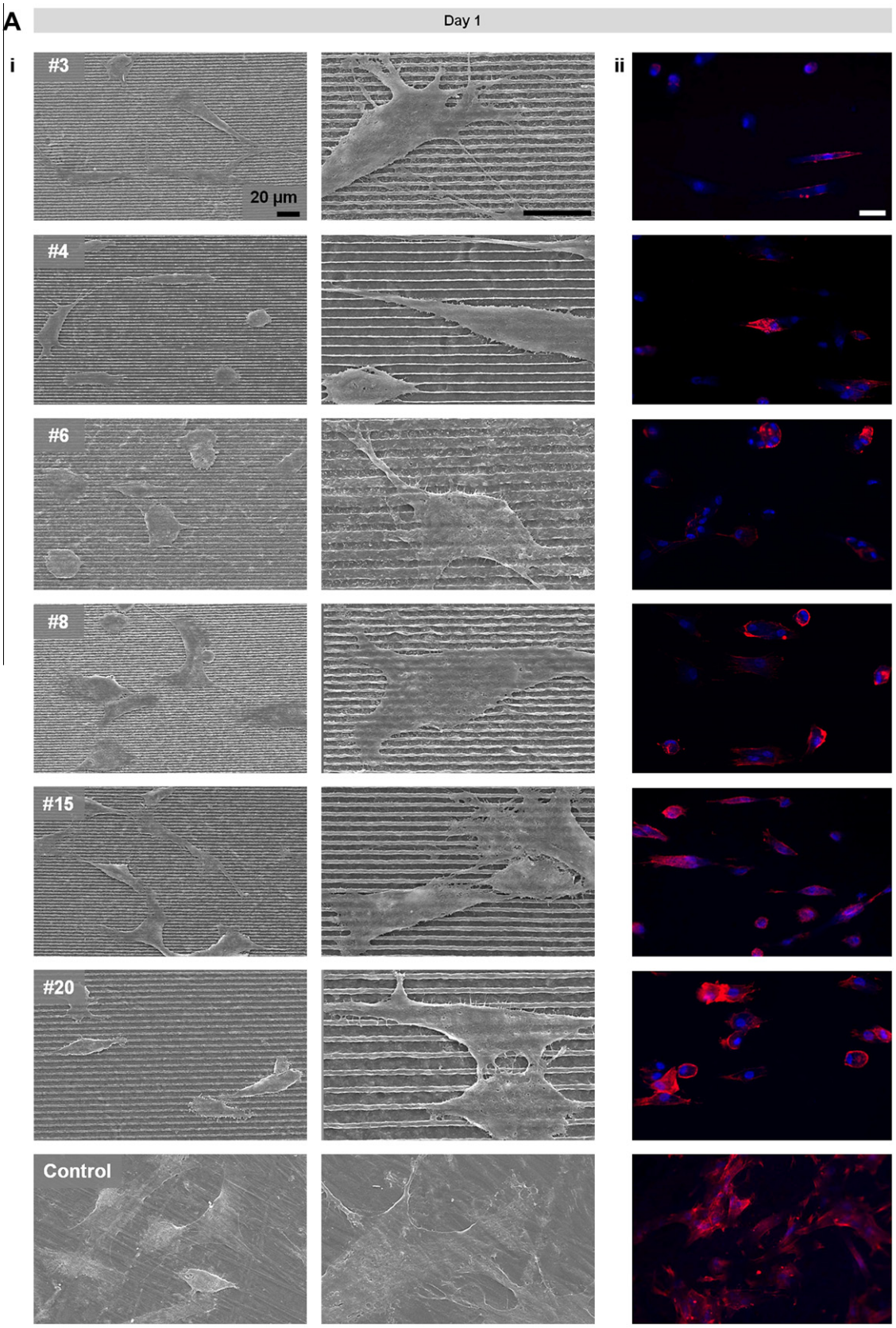

Fig. 6. SEM at two magnifications (i) and (ii) of immunostaining of hASCs cultured onto micropatterned PBS surfaces after (A) 1 day and (B) 3 days of culture: cell cytoskeleton stained red with phalloidin and cell nucleus counterstained blue with DAPI.

atures in a process resulting from the rearrangement of the cellular cytoskeleton [26,33,34] and that different cell types can sense the surface topography differently. Thus, although hASCs have aligned along the engineered micropatterned surfaces with a groove/ridge ratio bigger than 1, other cell types might have a different behavior.

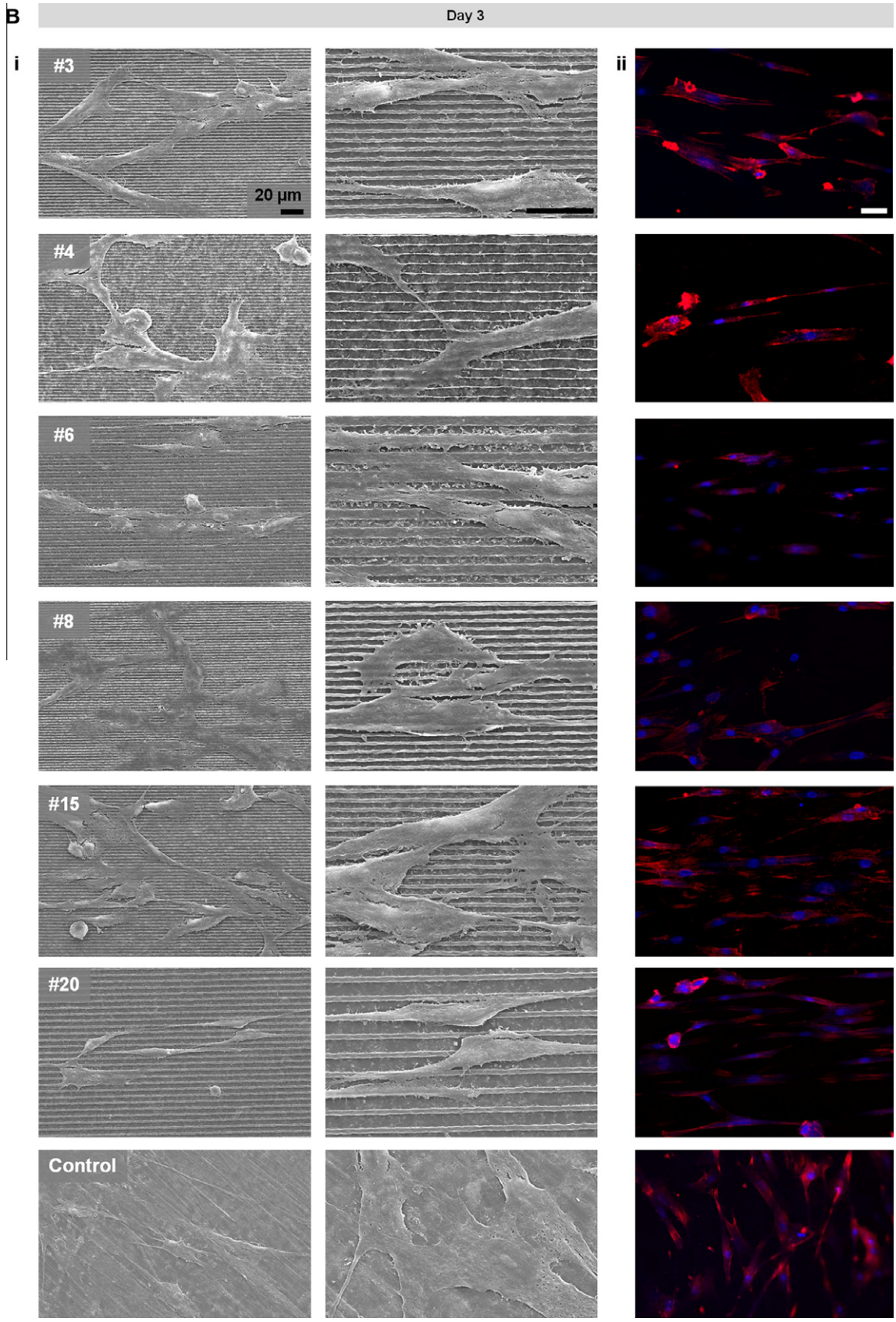

Fig. 6 (*continued*)

4. Conclusions

Micropatterned surfaces of the biodegradable polyester PBS were successfully microengineered by micromolding. The system parameters, namely the temperature of the mold and the solution, the polymer concentration, and the solvent used to dissolve the PBS pellets were optimized, allowing the development of a variety of micropatterns with different sizes of features. The combination of different groove and ridge sizes resulted in the microfabrication of 10 patterns with groove size higher than the ridge, 6 patterns with groove size smaller than the ridge size and 4 patterns with similar groove and ridge sizes. The in vitro biological behavior of selected biomimetic micropatterned surfaces revealed that the engineered surfaces were able to maintain a high viability of hASCs. The engineered surfaces appear to direct the orientation of seeded hASCs along the micropatterned features of PBS. In contrast, cells appear to be randomly oriented on the non-patterned surfaces. This study combines microtechnologies and biomaterials to engineer a biomimetic surface at the microlevel using a polyester that has been widely studied by our group. The importance of PBS microstructure for the attachment and morphology of hACS, a stem cell source with a high degree of multipotency, was demonstrated, indicating the potential of these surfaces as substrates for guided tissue engineering approaches.

Acknowledgements

This work was partially supported by the Foundation for Science and Technology (FCT), through funds from the POCTI and/or FEDER programs and from the European Union under the project NoE EXPERTISSUES (NMP3-CT-2004-500283). D.F.C. acknowledges the Foundation for Science and Technology (FCT), Portugal and the MIT-Portugal Program for personal grant SFRH/BD/37156/2007. The authors thank to Dr. Erkan Baran for scientific discussions and Professor Hong Hong Lee (Seoul National University) for providing the PDMS mold used in this study.

Appendix A. Figures with essential colour discrimination

Certain figures in this article, particularly Fig. 6, is difficult to interpret in black and white. The full colour images can be found in the on-line version, at doi:10.1016/j.actbio.2011.12.035.

References

[1] Aloy P, Russell RB. Structure-based systems biology: a zoom lens for the cell. Febs Lett 2005;579(8):1854–8.
[2] LeDuc PR, Bellin RM. Nanoscale intracellular organization and functional architecture mediating cellular behavior. Ann Biomed Eng 2006;34(1):102–13.
[3] Malmsten M. Formation of adsorbed protein layers. J Colloid Interface Sci 1998;207(2):186–99.
[4] Huang Y, Lu XY, Qian WP, Tang ZM, Zhong YP. Competitive protein adsorption on biomaterial surface studied with reflectometric interference spectroscopy. Acta Biomaterialia 2010;6(6):2083–90.
[5] Kawamoto N, Mori H, Terano M, Yui N. Blood compatibility of polypropylene surfaces in relation to the crystalline-amorphous microstructure. J Biomater Sci Polym Ed 1997;8(11):859–77.
[6] Weber N, Bolikal D, Bourke SL, Kohn J. Small changes in the polymer structure influence the adsorption behavior of fibrinogen on polymer surfaces: validation of a new rapid screening technique. J Biomed Mater Res A 2004;68A(3):496–503.
[7] Roach P, Farrar D, Perry CC. Surface tailoring for controlled protein adsorption: Effect of topography at the nanometer scale and chemistry. J Am Chem Soc 2006;128(12):3939–45.
[8] Papadaki M, Bursac N, Langer R, Merok J, Vunjak-Novakovic G, Freed LE. Tissue engineering of functional cardiac muscle: molecular, structural, and electrophysiological studies. Am J Phys Heart Circ Physiol 2001;280(1):168–78.
[9] Skedros JG, Dayton MR, Sybrowsky CL, Bloebaum RD, Bachus KN. The influence of collagen fiber orientation and other histocompositional characteristics on the mechanical properties of equine cortical bone. J Exp Biol 2006;209(15):3025–42.
[10] Fukuda J, Khademhosseini A, Yeh J, Eng G, Cheng JJ, Farokhzad OC, et al. Micropatterned cell co-cultures using layer-by-layer deposition of extracellular matrix components. Biomaterials 2006;27(8):1479–86.
[11] da Silva M, Martins A, Costa-Pinto A, Costa P, Faria S, Gomes M, et al. Cartilage tissue engineering using electrospun PCL nanofiber meshes and MSCs. Biomacromolecules 2010;11(12):3228–36.
[12] Santos MI, Tuzlakoglu K, Fuchs S, Gomes ME, Peters K, Unger RE, et al. Endothelial cell colonization and angiogenic potential of combined nano- and micro-fibrous scaffolds for bone tissue engineering. Biomaterials 2008;29(32):4306–13.
[13] Martins A, Pinho ED, Faria S, Pashkuleva I, Marques AP, Reis RL, et al. Surface modification of electrospun polycaprolactone nanofiber meshes by plasma treatment to enhance biological performance. Small 2009;5(10):1195–206.
[14] Khademhosseini A, Eng G, Yeh J, Kucharczyk PA, Langer R, Vunjak-Novakovic G, et al. Microfluidic patterning for fabrication of contractile cardiac organoids. Biomed Microdevices 2007;9(2):149–57.
[15] Baran ET, Tuzlakoglu K, Salgado A, Reis RL. Microchannel-patterned and heparin micro-contact-printed biodegradable composite membranes for tissue-engineering applications. J Tissue Eng Regenerative Med 2011;5(6):E108–14.
[16] Tserki V, Matzinos P, Pavlidou E, Vachliotis D, Panayiotou C. Biodegradable aliphatic polyesters Part I. Properties and biodegradation of poly(butylene succinate-co-butylene adipate).. Polym Degradation Stability 2006;91(2):367–76.
[17] Tserki V, Matzinos P, Pavlidou E, Panayiotou C. Biodegradable aliphatic polyesters Part II. Synthesis and characterization of chain extended poly(butylene succinate-co-butylene adipate). Polym Degradation Stability 2006;91(2):377–84.
[18] Correlo VM, Boesel LF, Bhattacharya M, Mano JF, Neves NM, Reis RL. Properties of melt processed chitosan and aliphatic polyester blends. Mater Sci Eng Struct Mater Properties Microstruct Process 2005;403(1–2):57–68.
[19] Pinto AR, Correlo VM, Bhattacharya M, Charbord P, Reis RL, Neves NM. Behaviour of human bone marrow mesenchymal stem cells seeded on fiber bonding chitosan polyester based for bone tissue engineering scaffolds. Tissue Eng 2006;12(4):1019.
[20] Costa-Pinto A, Correlo V, Sol P, Bhattacharya M, Srouji S, Livne E, et al. Chitosan–poly(butylene succinate) scaffolds and human bone marrow stromal cells induce bone repair in a mouse calvaria model. J Tissue Eng Regenerative Med 2011.
[21] da Silva MLA, Crawford A, Mundy JM, Correlo VM, Sol P, Bhattacharya M, et al. Chitosan/polyester-based scaffolds for cartilage tissue engineering: Assessment of extracellular matrix formation. Acta Biomaterialia 2010;6(3):1149–57.
[22] Rada T, Reis RL, Gomes AE. Novel method for the isolation of adipose stem cells (ASCs). J Tissue Eng Regenerative Med 2009;3(2):158–9.
[23] Suh KY, Lee HH. Capillary force lithography: large-area patterning, self-organization, and anisotropic dewetting. Adv Funct Mater 2002;12(6–7):405–13.
[24] Suh KY, Kim YS, Lee HH. Capillary force lithography. Adv Mater 2001;13(18):1386–9.
[25] Khang DY, Lee HH. Pressure-assisted capillary force lithography. Adv Mater 2004;16(2):176–9.
[26] Teixeira AI, Nealey PF, Murphy CJ. Responses of human keratocytes to micro- and nanostructured substrates. J Biomed Mater Res A 2004;71A(3):369–76.
[27] Khetan S, Burdick JA. Patterning network structure to spatially control cellular remodeling and stem cell fate within 3-dimensional hydrogels. Biomaterials 2010;31(32):8228–34.
[28] Charest JL, Garcia AJ, King WP. Myoblast alignment and differentiation on cell culture substrates with microscale topography and model chemistries. Biomaterials 2007;28(13):2202–10.
[29] Hohn FJ. Electron-beam lithography-tools and applications. Jpn J Appl Phys 1 1991;30(11B):3088–92.
[30] Newnam BE. Extreme ultraviolet free-electron laser-based projection lithography systems. Opt Eng 1991;30(8):1100–8.
[31] Rada T, Reis RL, Gomes ME. Adipose tissue-derived stem cells and their application in bone and cartilage tissue engineering. Tissue Eng Part B Rev 2009;15(2):113–25.
[32] Zuk PA, Zhu M, Mizuno H, Huang J, Futrell JW, Katz AJ, et al. Multilineage cells from human adipose tissue: Implications for cell-based therapies. Tissue Eng 2001;7(2):211–28.
[33] Flemming RG, Murphy CJ, Abrams GA, Goodman SL, Nealey PF. Effects of synthetic micro- and nano-structured surfaces on cell behavior. Biomaterials 1999;20(6):573–88.
[34] Rebollar E, Frischauf I, Olbrich M, Peterbauer T, Hering S, Preiner J, et al. Proliferation of aligned mammalian cells on laser-nanostructured polystyrene. Biomaterials 2008;29(12):1796–806.